

# Tubular silk scaffolds for small diameter vascular grafts

Michael Lovett<sup>1,†</sup> George Eng,<sup>2,†</sup> Jonathan A. Kluge,<sup>1</sup> Christopher Cannizzaro,<sup>1</sup> Gordana Vunjak-Novakovic<sup>2,\*</sup> and David L. Kaplan<sup>1</sup>

<sup>1</sup>Department of Biomedical Engineering; Tufts University; Medford, MA USA; <sup>2</sup>Department of Biomedical Engineering; Columbia University; New York, NY USA

<sup>†</sup>These authors contributed equally to this work.

**Key words:** vascular graft, blood vessels, silk, tissue engineering

Vascular surgeries such as coronary artery bypass require small diameter vascular grafts with properties that are not available at this time. Approaches using synthetic biomaterials have not been completely successful in producing non-thrombogenic grafts with inner diameters less than 6 mm, and there is a need for new biomaterials and graft designs. We propose silk fibroin as a microvascular graft material and describe tubular silk scaffolds that demonstrate improved properties over existing vascular graft materials. Silk tubes produced using an aqueous gel spinning technique were first assessed in vitro in terms of thrombogenicity (thrombin and fibrinogen adsorption, platelet adhesion) and vascular cell responses (endothelial and smooth muscle cell attachment and proliferation) in comparison with polytetrafluoroethylene (PTFE), a synthetic material most frequently used for vascular grafts. Silk tubes were then implanted into the abdominal aortas of Sprague-Dawley rats. At time points of 2 weeks and 4 weeks post-implantation, tissue outcomes were assessed through gross observation (acute thrombosis, patency) and histological staining (H&E, Factor VIII, smooth muscle actin). Over the 4-week time period, we observed graft patency and endothelial cell lining of the lumen surfaces. These results demonstrate the feasibility of using silk fibroin as a vascular graft material and some advantages of silk tubes over the currently used synthetic grafts.

## Introduction

With the constant increase in the incidence of atherosclerosis, there is a need for small vascular grafts (<6 mm inner diameter, ID) for vascular surgeries such as coronary or femoral artery bypass. Clinically, the current “gold standard” is autologous grafting, where the saphenous vein or an internal mammary artery is used to bypass the diseased vessel.<sup>1</sup> Unfortunately, in patients who have had previous bypass surgeries or vascular disease, the veins and arteries are often unsuitable for harvest.<sup>2</sup> In addition, the need to generate a second surgical site can lead to greater risk of infection, swelling and discomfort. Thus, there is a long-standing need to develop a functional alternative to autologous grafting.

Currently available synthetic grafts, such as expanded polytetrafluoroethylene (PTFE, Teflon<sup>®</sup>) and polyethylene terephthalate (PET, Dacron<sup>®</sup>), are successful at the macrovascular level, but fail at smaller diameters (<6 mm ID) due to thrombosis and/or compliance mismatches.<sup>3-5</sup> Because this is the actual scale of interest for coronary and femoral artery bypass procedures, numerous chemical and physical modification techniques have been developed and applied to synthetic grafts to tailor the materials to achieve a desired bioactivity and biocompatibility. These techniques include chemical grafting of functional groups,

plasma surface modifications and physical adsorption of coatings, typically using an anticoagulant such as heparin.<sup>6-9</sup> These methods, however, are limited due to complexity of processing, loss of activity of biomolecules delivered within these coatings, and the lack of control of the spatial distribution of the material. In addition, most of these biomaterials are non-degradable, a feature known to prevent full restoration of the original tissue structure and function.

The need for new biomaterials and approaches to generate functional small diameter vascular grafts with capacity for remodeling remains. The design criteria are stringent, in particular with respect to mechanical competence, non-thrombogenicity and ability to remodel over time into a fully functional blood vessel. Additional requirements include biocompatibility, biodegradation, mechanical compliance, precise geometry, suturability, non-immunogenicity and possible translation into pre/clinical studies. To address these challenges, we propose to use a natural biopolymer—silk fibroin, which offers robust and tailorable mechanical properties along with biocompatibility, slow degradation in vivo and versatile processing options to permit the formation of small diameter tubular systems.<sup>5,10</sup>

To this end, aqueous silk solutions were spun using a custom-designed gel spinning technique for producing small diameter

\*Correspondence to: Gordana Vunjak-Novakovic; Email: gv2131@columbia.edu

Submitted: 07/10/10; Revised: 08/23/10; Accepted: 08/25/10

Previously published online: [www.landesbioscience.com/journals/organogenesis/article/13407](http://www.landesbioscience.com/journals/organogenesis/article/13407)

DOI: 10.4161/org6.4.13407

tubular conduits with fine control over tube properties (mechanics, lifetime, structural features).<sup>10</sup> In the present study, the focus was placed on using lyophilized silk tubular grafts that have a long shelf life, can be designed to achieve structural and mechanical compliance and to control vascular cell migration and proliferation. Lyophilized silk material was evaluated in terms of mechanical strength, thrombogenic potential (by measuring thrombin and fibrinogen adsorption and platelet adhesion) and endothelial and smooth muscle cell attachment and proliferation. Measured data were compared to PTFE tubes.

Silk grafts were then implanted into the abdominal aorta of Sprague-Dawley rats by end-to-end anastomosis and evaluated for signs of acute thrombosis. The grafts were harvested at two and four weeks post-implantation to evaluate patency, migration and proliferation of smooth muscle cells and the formation of confluent endothelium. This work suggests that silk may be a suitable material for small diameter vascular grafts and that the problems with thrombosis and compliance (structural and mechanical) can be addressed through the structural and mechanical graft design.

## Results and Discussion

**Silk tubes structure.** A silk gel spinning approach was used to form tailored silk tubes with tight control of winding parameters and post-winding processing techniques over a wide range of structural properties (Fig. 1). This was achieved by depositing silk onto a reciprocating rotating mandrel, controlling the rate of rotation and axial slew and subjecting the tubes to methanol treatment, air-drying and lyophilization before removal from the mandrel (Fig. 1A–C). We previously reported the technique developed for manufacturing the silk tubes, the various geometries that can be made using these techniques and the structural and mechanical properties of silk tubes.<sup>5,10</sup>

In this study, silk tubes were produced using a simple wrapping pattern and lyophilized post-winding to obtain a highly porous, lamellar-like structure (Fig. 1D–G). Compared to silk tubes obtained by other variations of the process, the lyophilized tubes display an increased surface roughness and porosity, allowing for potential cell in-growth. Also, the lyophilized tubes are more flexible, a critical parameter for a vascular graft.

**Mechanical properties of vascular graft materials.** Structural properties of silk, PTFE tubes and native rat abdominal aortas were evaluated by measuring the values of the elastic modulus and ultimate tensile strength in tensile testing. Major differences were observed in the stress-strain behavior of these materials. While the replacement materials (PTFE and silk) had a linear-elastic behavior in the low-strain regime, leading to a large zone of plastic deformation, the rat aorta displayed a “toe region” directly preceding the more linear behavior (from which the elastic modulus was extracted).<sup>21</sup> This toe region can be attributed to the straightening and alignment of elastin fibers, a mechanism that regulates the compliance of blood vessels during normal systolic and diastolic pressures.

As shown in Table 1, both the elastic modulus and ultimate tensile strength are orders of magnitude higher for the PTFE

tubes than for silk tubes, indicating that the PTFE is a stronger, stiffer material. Notably, silk tubes matched much more closely the mechanical properties of rat abdominal aorta. While the properties of PTFE may be suitable for grafts used to treat large diameter arteries where blood flow is higher and the resistance is low, this mismatch in mechanical strength between PTFE and native vessels at smaller diameters can lead to low patency rates.<sup>22</sup> In contrast, silk tubes display mechanical properties that more closely match those of the rat aorta and human saphenous vein,<sup>23–25</sup> raising the possibility that by more closely matching the compliance properties of small diameter vessels, thrombogenicity can be reduced.

Matching of the mechanical properties was used as an a priori design evaluation tool given that the compliance mismatch at points of anastomosis was suggested as primary causes of thrombosis. While the toe region behavior was not prioritized, this behavior can be accommodated as necessary by incorporating criss-cross fibrillar winding patterns typical of textile-based structures. Radial compliance and the tube burst pressure can also be regulated through careful modifications to the silk tube making process. Previous work using electrospun or aqueous-dipped silk tubes has demonstrated that silk tubes have sufficient mechanical properties to withstand physiological blood pressures.<sup>5,26</sup>

**Thrombogenic potential of silk and PTFE.** Evaluation of the thrombogenic potential of silk compared to other materials was performed by observing the amount of thrombin and fibrinogen adsorption to silk and PTFE and by comparing platelet adhesion and spreading on silk as compared to PTFE, collagen, glass and glass coated with bovine serum albumin (BSA) (Fig. 2). Thrombin and fibrinogen were chosen for these adsorption studies for their respective roles in the common thrombogenic pathway. The proteins were biotinylated to quantitatively assess the amount of protein adsorbed to each surface and concentrations of each protein (0–5 µg/mL) were deposited onto the silk and PTFE films as well as Maxisorp plates as a control. As shown in Figure 2A and B, there was a dose-dependent response of the protein adsorbed by the films for both the biotinylated thrombin and fibrinogen. The amount of protein adsorbed onto the silk films was lower than that of the PTFE films for all cases, indicating that silk may be less thrombogenic in vivo as compared to PTFE.

The mechanism of protein adsorption may be associated with hydrophobic interactions between the protein and the film, as contact angles of silk and PTFE have been reported to be approximately 79–83° and 95–105°, respectively.<sup>27,28</sup> The relatively small increase in hydrophobicity of the PTFE as compared to the silk may account for the slight increase in protein adsorption. Still, both surfaces adsorbed only small amounts of protein (<5 ng per sample) compared to the total amount of protein loaded onto the film (0.05 to 0.5 µg).

Thrombogenic potential of the graft materials was also evaluated by measuring platelet adhesion and spreading on silk and PTFE. These data were compared to data obtained for other control films and surfaces. Platelet-rich plasma was incubated on silk, PTFE and collagen films, with glass and glass coated with 0.5% bovine serum albumin (BSA) serving as the positive and

negative controls, respectively.<sup>29</sup> As shown in **Figure 2C and D**, PTFE demonstrated the lowest level of platelet adhesion, as compared to silk and collagen films. Platelet adhesion to BSA-coated glass was higher than that to unmodified glass. A similar level of spreading was observed for platelets attached to silk and PTFE (**Fig. 2D**). The platelets displayed a non-spreading morphology when in contact with silk and PTFE, similar to that normally found for collagen and BSA-coated glass substrates, indicative of a non-activated phenotype.<sup>30</sup> By demonstrating platelet morphology close to those found on surfaces known to not activate platelets (collagen, BSA-coated glass), silk and PTFE surfaces were thus expected to be relatively non-thrombogenic.

**Characterization of vascular cell attachment and proliferation.** In order to assess the ability of silk tubes to remodel and integrate in vivo, we first investigated the attachment and proliferation of endothelial and smooth muscle cells in vitro. The ability of these cells to grow on silk films in vitro was compared to PTFE, collagen films and tissue culture plastic (TCP), to get insights into cell migration and adherence. As shown in **Figure 3A and B**, the attachment to silk films of both the endothelial cells (HUVECs) and smooth muscle cells (SMCs) was higher than that observed for PTFE. This suggests a higher potential of silk grafts for the formation of endothelial cell lining on the inner surface of the graft lumen and graft remodeling by the infiltrating SMCs. In this respect, the PTFE material is more inert and has more limited ability for cell integration. However, both the silk and PTFE films showed dramatic reduction of cell binding compared to collagen films or TCP, suggesting that these two graft materials can provide cell attachment and infiltration necessary for remodeling while limiting thrombotic factor attachment that can lead to vessel occlusion.

The ability of cells to proliferate on silk and PTFE was assessed using a PicoGreen dsDNA assay, over a two week time period. The rate of cell proliferation on the silk films fell between the values measured for TCP and PTFE. This implies that vascular cells (HUVECs, SMCs) may proliferate on silk in a way not observed on standard PTFE (**Fig. 3C and D**). Actively proliferating cells may remodel the silk graft in parallel with silk degradation and ultimately result in a fully remodeled graft with the same properties as the native vessel. The progression of remodeling may be further controlled by varying silk processing and by mediating vascular cell proliferation by loading with therapeutic compounds such as paclitaxel, heparin and clopidogrel.<sup>11</sup>

**Preliminary in vivo evaluation of silk tubes.** Using an abdominal aorta implantation model in rats, silk tubes were evaluated in vivo for their potential as a vascular graft material. The rats exhibited no signs of acute thrombosis (within 24 hours), and were monitored throughout the study (within one month) for any signs of occlusion, clotting or ischemia. At 2 weeks and 4 weeks following implantation, the grafts and adjacent native blood vessels were harvested for histological evaluation. Serial cross-sections at various positions along the graft were assessed using H&E staining for overall evaluation as well as markers for endothelial and smooth muscle cells (**Fig. 4**).

The ability of the lyophilized silk tubes to remain patent was particularly encouraging, given that small diameter PTFE tubes

implanted in parallel exhibited occlusion within 24 hours. These preliminary animal studies indicate the migration of host cells into the grafts along with the maintenance of graft patency over a period of up to 4 weeks. Specifically, the host SMCs populated the interior of the graft walls, and the host ECs formed the endothelial cell lining at the inner lumen surfaces (**Fig. 4**). The evidence of medial smooth muscle cells inside the graft walls and confluent endothelium was seen by smooth muscle actin (SMA) and factor VIII staining (**Fig. 4**). A recent animal study of similar silk tube grafts (1.5 mm in inner diameter, 10 mm in length) also reports excellent patency over a period of 12 months, associated with the migration of endothelial cells and smooth muscle cells into the silk fibroin graft.<sup>31</sup>

Graft cellularity increased with time in vivo, suggesting the progressive migration and proliferation of SMCs and ECs from the adjacent native aorta. Direct comparison of the amounts of Factor VIII in the distal section of the graft at 2 weeks and 4 weeks post implant shows remarkable remodeling and resorption of the initial thrombotic laminations, resulting in a neat and confluent endothelial cell layer. Cells proliferated throughout the length of the silk graft and were adherent to the walls of the tube at the time of harvest. It is especially interesting that the silk tubes remained patent without any special modifications or incorporation of drugs.

Potential SMC hyperproliferation hyperplasia over longer times and in future, more peripheral arterial studies, however, may necessitate stricter control over the properties of the silk tubes. The all-aqueous nature of the gel spinning process allows for incorporation of specific anti thrombotic target factors (e.g., paclitaxel, heparin, warfarin, aspirin or clopidogrel) directly into the tubes to regulate cell and protein response.<sup>17,18</sup> Previous work in our lab has focused on the incorporation of paclitaxel, a vascular smooth muscle inhibitor commonly found in drug-loaded stents<sup>19,20</sup> and shown in previous studies using silk to inhibit smooth muscle cell proliferation.<sup>11</sup> By incorporating different doses (10 µg/mL to 1 mg/mL) of paclitaxel into the tubes during the silk spinning process, smooth muscle cell proliferation may be regulated as shown in previous work.<sup>11</sup>

## Materials and Methods

**Silk tube manufacture.** Silk fibroin aqueous solutions were obtained from *Bombyx mori* silkworm cocoons using previously described procedures.<sup>10</sup> Briefly, the silkworm cocoons (supplied by Tajima Shoji Co., LTD., Yokohama, Japan) were extracted in 0.02 M sodium carbonate solution, rinsed in distilled water, dissolved in 9.3 M lithium bromide and dialyzed against distilled water using a Slide-a-Lyzer dialysis cassette (molecular weight cutoff MWCO, 3,500, Pierce, Rockford, IL) for 48 hours. The resulting 6–8% (w/v) fibroin solution was then concentrated by dialyzing against 10 wt% poly(ethylene glycol) (PEG) to produce a 25–35% (w/v) silk fibroin aqueous solution.

Tubes were prepared by using a previously described gel spinning approach, at conditions resulting in silk tubes with structural and mechanical compliance similar to that of the rat abdominal aorta.<sup>10</sup> Briefly, a concentrated silk fibroin solution [–25–35%



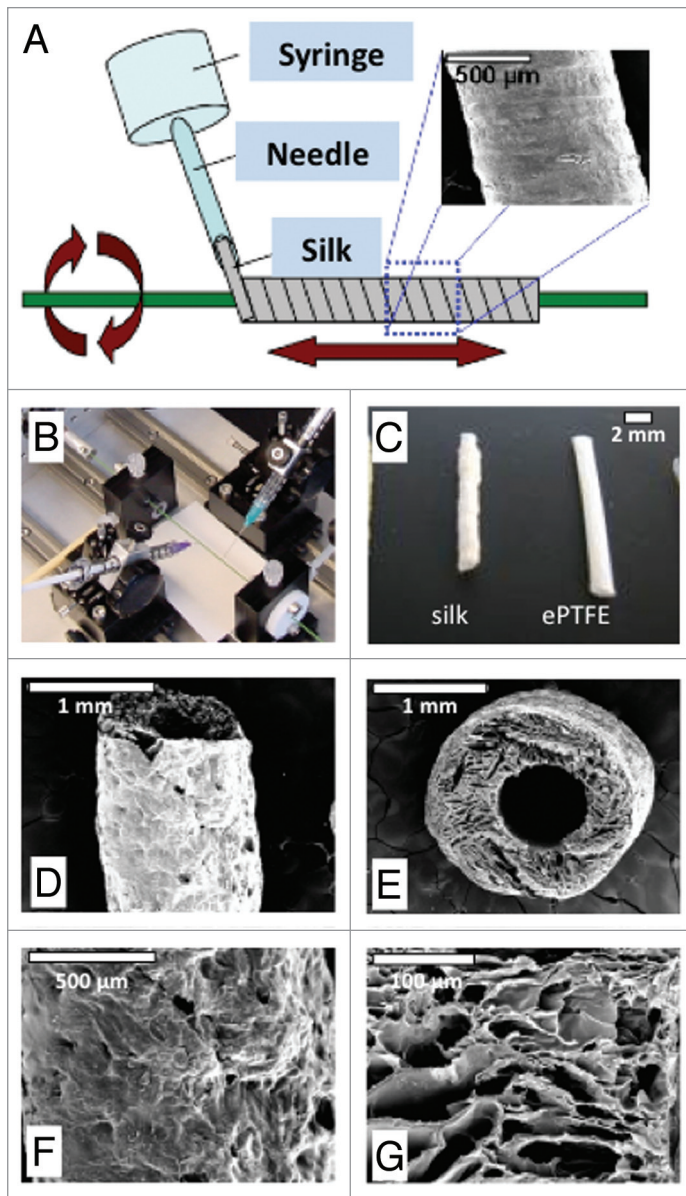


**Figure 1.** Silk fibroin vascular grafts. (A) Schematics of gel spinning process used to produce silk tubes where a concentrated silk solution is expelled through a small gauge needle and wound onto a rotating reciprocating mandrel. (B) Image of the gel spinning apparatus; (C) images of grafts compared in this study, silk and ePTFE; SEM images of silk tubes both longitudinally (D and F) and in cross-section (E and G).

**Table 1.** Comparison of structural properties of native aorta and graft material

	Elastic modulus (MPa)	Ultimate tensile strength (MPa)
Native rat aorta	2.44 ± 0.76	0.519 ± 0.11
Silk tube	2.20 ± 0.90	0.273 ± 0.11
PTFE tube	918 ± 52.9	43.4 ± 4.6

(w/v) was driven through a 27 or 30 gauge needle onto a rotating and axially reciprocating mandrel. After evenly coating the mandrel with the concentrated silk fibroin using a desired winding pattern, the tubes were frozen and lyophilized. After brief treatment with methanol, the silk-coated mandrel was placed in a surfactant solution and the silk tube was removed from the Teflon-coated stainless steel rod. This previously established method was used to make silk tubes matching the size of abdominal aorta in Sprague-Dawley rat (inner diameter 1.0–1.5 mm, length 20 mm, wall thickness 0.1 mm).

**Mechanical testing of graft materials.** Tensile tests were performed on hydrated silk tubes and PTFE as previously described.<sup>10</sup> Briefly, an Instron 3366 testing frame with a 10 N capacity load cell and Biopuls pneumatic clamps was used to test the sample tubes (sample size N = 3–5). The tubes used for mechanical testing were 1.5 ± 0.05 mm inner diameter and with a wall thickness of 0.1 ± 0.03 mm. The length of samples was measured using a caliper (20–30 mm) and the tubes were hydrated in 0.1 M phosphate-buffered saline (PBS) for approximately 30 minutes before clamping. Prior to testing, all samples were submerged in temperature-controlled Biopuls bath (37 ± 0.3°C) filled with 0.1 M PBS (Sigma) for 5 minutes.

A crosshead displacement rate of 5 mm/min was used and the measured tensile stress was plotted against tensile strain. The elastic modulus was calculated using a least-squares fit in the linear range of the stress-strain plot. The yield strength was determined by offsetting the least-squares line by a strain of 2% (silk) or 0.2% (PTFE). Ultimate tensile strength was measured as the highest stress value attained during the test. The elongation to failure was measured as the last data point before a >10% decrease in the load was observed.

**Protein adsorption to silk and PTFE films.** Protein adsorption to silk films and PTFE was measured using thrombin and fibrinogen, proteins of the common thrombotic pathway. Silk and PTFE films were deposited into wells of Maxisorp plates (Nunc Brand, Fisher Scientific, Rochester, NY) after blocking the wells with 1% BSA in PBS-Tween solution (0.05% Tween 20 in PBS). Silk films were made by pipetting 50 μL of 6–8% silk solution into each well, letting the solution dry overnight, and treating with 70% methanol. PTFE films were made by coring out 6 mm diameter circles out of the PTFE sheet (0.05 mm thick, McMaster-Carr, Robbinsville, NJ), by using a biopsy punch. The films were held in place by a small amount of medical device adhesive (Loctite® 4013).

In order to quantify protein adsorption to silk and PTFE films, each protein was biotinylated using an EZ-Link NHS-Chromogenic Biotinylation Kit (Pierce, Rockford, IL). An amine-reactive NHS ester was coupled to a chromogenic group, a polyethylene glycol (PEG) spacer and a biotin group. This reagent was used to react to the primary amino groups on the proteins of interest, forming stable amide bonds and allowing for quantification of biotin incorporation through the use of the incorporated chromophore.

Varying concentrations of these biotinylated proteins (0 to 5 μg/mL) were incubated overnight at 4°C on silk and PTFE films and on uncoated Maxisorp plates (100 μL/well).

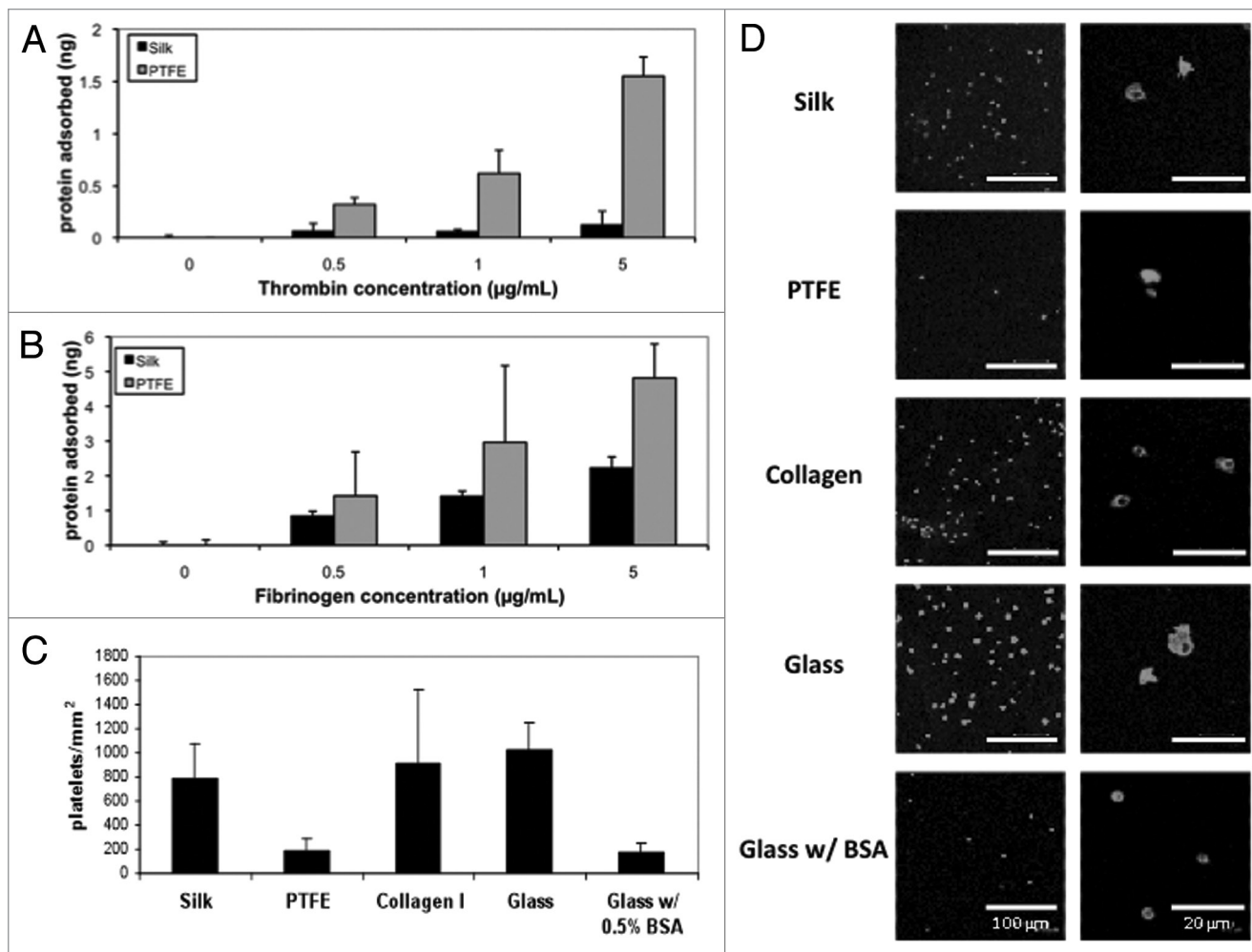


**Figure 2.** Characterization of thrombogenic potential of different materials. Adsorption of biotinylated thrombotic pathway proteins thrombin (A) and fibrinogen (B) to silk fibroin and PTFE films. Protein concentrations on each film ranged from 0 to 5 µg/mL and protein adsorption to the films was quantified using an ELISA technique. Platelet adhesion after 30 minute incubation quantified in terms of platelets per square millimeter (C) with images of platelets adherent to the different materials (D).

Adsorption was evaluated using an enzyme-linked immunosorbent assay (ELISA)-based technique, as described previously.<sup>12</sup> Briefly, after incubation, wells were washed with PBS-Tween and blocked with 1% BSA in PBS-Tween to inhibit non-specific binding. After incubation, the plate was washed again with PBS-Tween before adding horseradish peroxidase (HRP)-conjugated streptavidin. After an additional incubation and washing step, TMB was added to each well, incubated until sufficient color development, quenched by addition of 2 N sulfuric acid and transferred to a fresh plate for reading absorbance at 450 nm using a microplate reader. Absorbance values for the different concentrations of biotinylated proteins on silk and PTFE films were compared to the absorbance values for different concentrations on a standard curve on the uncoated Maxisorp plate.

**Cell culture.** Human coronary artery smooth muscle cells (HCASMCs), human umbilical vein endothelial cells (HUVECs) and a GFP-expressing line of HUVECs (GFP-HUVECs) were used to evaluate silk graft material.<sup>12</sup> Prior to

seeding, the cells were cultured according to previously reported protocols, as follows. HUVEC cells were grown in optimized growth media EGM-2 (Lonza, Walkersville, MD) supplemented with 100 U/mL penicillin, 1,000 U/mL streptomycin and 0.2% fungizone antimycotic (GIBCO, Carlsbad, CA). HCASMCs were cultured in smooth muscle cell medium (SMCM) with 2% fetal bovine serum (FBS), 1% smooth muscle cell growth supplement and 1% penicillin/streptomycin solution (ScienCell Research Laboratories, Carlsbad, CA). In some cases, prior to cell seeding, HCASMCs were stained using a red CellTracker dye at a concentration of 10 µM according to company protocols (Invitrogen, Carlsbad, CA).

**In vitro characterization of vascular cell attachment and proliferation and platelet adhesion.** The cellular components of thrombosis, vascular cell attachment and proliferation as well as platelet adhesion, were first assessed on films. Initial cell adhesion was monitored under a fluorescence microscope, for GFP-transduced HUVECs or HCASMCs labeled by the CellTracker dye. The numbers of cells were counted using ImageJ software.

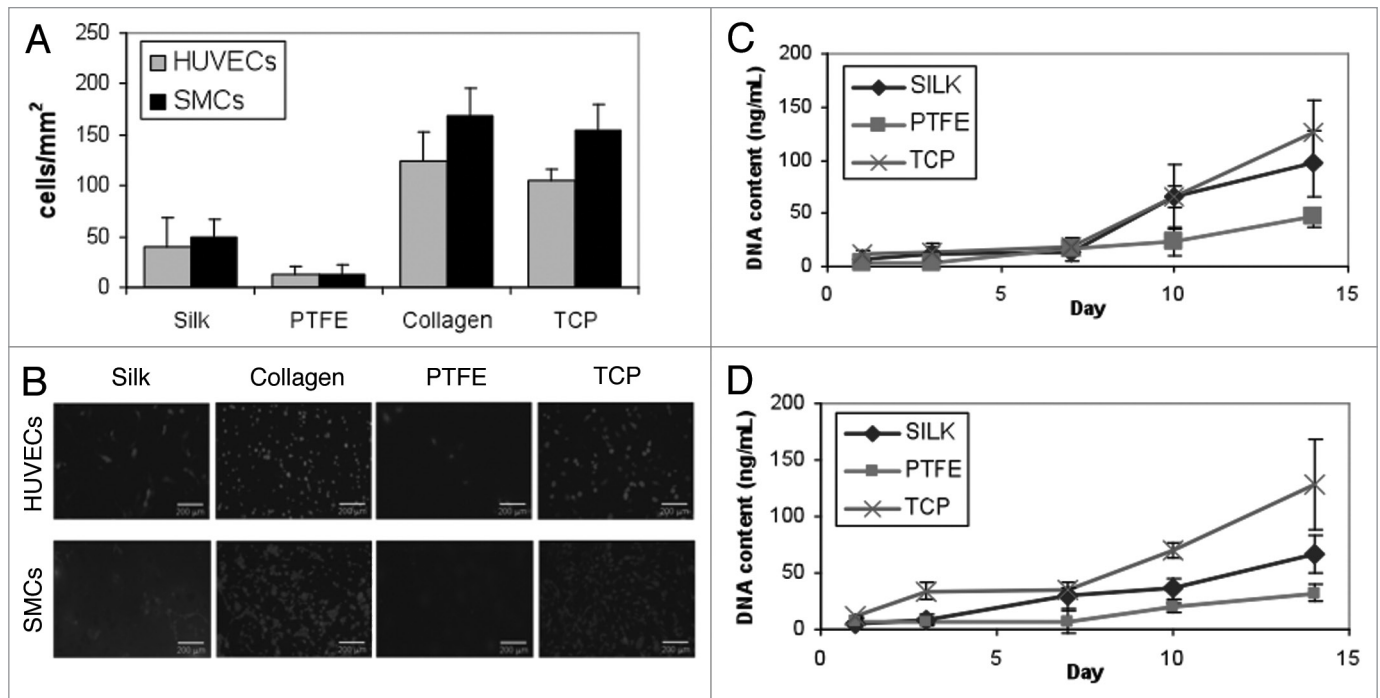


**Figure 3.** Characterization of vascular cell response to materials in vitro. (A) Endothelial and smooth muscle cell attachment after overnight incubation. (B) Images of HUVECs and SMCs on silk, collagen and PTFE films as well as tissue culture plastic (TCP) after overnight incubation. (C) Smooth muscle cell proliferation over two weeks. (D) Endothelial cell proliferation over a period of two weeks.

To assess cellular proliferation, HCASMCs and HUVECs were seeded onto the silk and PTFE films in a 24-well plate ( $2 \times 10^4$  cells/well). The DNA content in culture wells was measured every 3–4 days over the course of two weeks using a PicoGreen dsDNA assay (Invitrogen). Growth curves of the cells grown on silk and PTFE were compared with the cells grown on tissue culture plastics (positive control).

Platelets were obtained from platelet rich plasma (Research Blood Components), diluted in PBS to  $1 \times 10^7$  cells/mL and incubated on films for 30 minutes before washing, fixing and staining using CD61<sup>+</sup> antibody. After incubation, the films were washed 3 times with PBS to remove non-adherent platelets and fixed in 4% formalin for 20 minutes. After another series of PBS washes, adherent platelets were stained using monoclonal antibody CD61 (Beckman Coulter, Fullerton, CA) as the primary antibody and Alexa Fluor 488 chicken anti-mouse IgG as the secondary antibody (Invitrogen). Platelets were visualized using confocal microscopy and the number of adherent platelets was determined using ImageJ software.

**Scanning electron microscopy (SEM) and fluorescent microscopy of silk films and tubes.** SEM and fluorescence microscopy were used to visualize the surface morphology of the silk tubes or silk films and evaluate cell and platelet attachment, respectively. Tube samples for SEM were sputter-coated with gold using a Polaron SC502 Sputter Coater (Fisons, VG Microtech, East Sussex, England) and imaged using a JEOL JSM-840 Scanning Microscope (JEOL Ltd., Tokyo, Japan). Fluorescence images of the silk films were acquired using a Leica DMIRE2 confocal microscope with a TCS SP2 scanner

(Leica Microsystems, Mannheim/Wetzlar, Germany). PTFE tubes were imaged for comparison using the same methods.

**Graft implantation.** Silk tubes were implanted in the abdominal aorta of Sprague-Dawley rats via an end-to-end anastomosis model.<sup>13,14</sup> All procedures were performed according to an institutionally approved protocol. Prior to surgery, the silk tubes were adjusted to meet the anatomical requirements of the rats (1.0–1.5 mm inner diameter, 0.1 mm wall thickness, 20 mm length) and the rats were heparinized to help prevent thrombosis. The surgical model involved a midline laparotomy and subsequent exposure of the infrarenal abdominal aorta. Microclamps were used to halt blood flow and the aorta was transected and washed with saline. The silk graft was then interposed after necessary trimming of the adventitia into the native aorta and secured by 8–0 monofilament polypropylene sutures (total of 12). Target ischemia was within 30–60 minutes and graft patency was acutely assessed using a blanching flow-no flow technique before closing the animal. The rats were sacrificed after two or four weeks and the grafts were evaluated histologically, by staining segments of the grafts using hematoxylin and eosin (H&E) for general evaluation, Masson's trichrome for collagen, an antibody for smooth-muscle actin and factor VIII for endothelium.

**Structural comparison of graft materials.** To compare the structural properties of replacement tubes (silk and PTFE) to the native tissue site, the sections of transected rat aortas were looped several times by polypropylene sutures and left in PBS. Samples were anchored to steel hooks via sutures and submerged in temperature-controlled Biopuls bath ( $37 \pm 0.3^\circ\text{C}$ ) filled with 0.1 M PBS (Sigma) for 5 minutes prior to testing. After 5 minutes



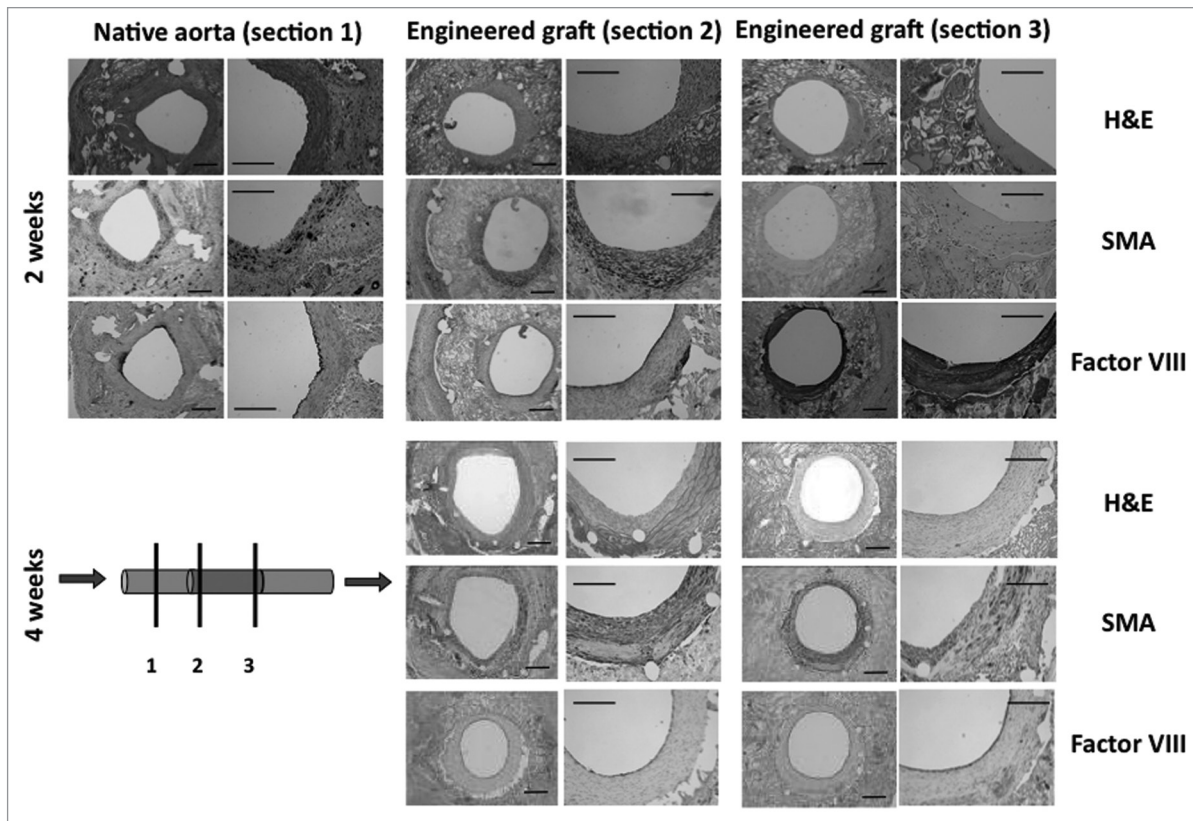


**Figure 4.** Histology of silk tube graft 2 weeks and 4 weeks post-implantation. Full cross-sections were taken at 2 weeks and 4 weeks post-implant for the native aorta (section 1, close to the interface with the silk tube) and at two different positions along the implanted silk tube graft (section 2 and section 3), as shown on the schematics. Blood flow is from left to right. Adjacent histological sections were stained for hematoxylin and eosin (H&E), smooth muscle actin (SMA) and Factor VIII at both time points. All images are shown in low and high magnification. After 2 weeks, silk grafts were patent with evidence of neointimal hyperplasia (see 2-week histologies of section 2) and a confluent endothelium (see 2-week histologies of section 3). After 4 weeks, these changes were less pronounced and tissue remodeling has taken place (see 4-week histologies of sections 2 and 3). All scale bars are 200  $\mu\text{m}$ .

was complete, the sample was straightened by eye and the load was tared. During the test, a displacement control mode was used, with a crosshead displacement rate of 5 mm/min. The initial gauge length was measured as the suture-suture distance and the original cross sectional area determined by histology (H&E staining). The gauge length was corrected in post-processing by normalizing to a 0.05 N preload for each sample, and this load was thereby extracted from the data set (0.05 N = 2–3% of the maximum breaking load seen during testing). The tensile stress ( $\sigma$ ) and strain ( $\epsilon$ ) were graphed and ultimate tensile strength determined from the processed data, defined as the highest stress value attained during the test. This value is equivalent to the suture pull-out retention capacity of the tissue. The elastic modulus was established by curve-fitting the stress-strain data to an exponential stiffening constitutive model using MatLAB software.<sup>15,16</sup> The constitutive equation has the form  $\sigma = A[\exp(B\epsilon) - 1]$  and has been used previously to model cartilage, meniscus and ligament tissues (other collagen-fiber reinforced tissues). Parameters  $A$  and  $B$  were found using a least-squares minimization technique. The derivative of this equation is  $E = B\epsilon + C$  where  $C$  is the product of  $AB$  and  $E$  is the tangent elastic modulus. The elastic modulus was calculated at a stress value 0.2 MPa

(using the corresponding strain value), which objectively captured the linear portion of the stress-strain data for every sample.

## Conclusions

Small diameter silk tubes offer promise as a vascular graft, and could provide a good alternative to existing nondegradable grafts. Through the use of a natural biopolymer, silk fibroin and a gel spinning technique, silk tubes can be produced with precise control over dimensions, micro- and macro-structure, mechanical properties and drug loading and release. Silk grafts thus offer improvements over synthetic grafts in terms of biodegradability, vascular cell remodeling and control of material deposition and function (both chemical and mechanical).

Silk fibroin favorably compares to PTFE in terms of thrombogenicity, as demonstrated by untreated silk graft patency over the period of up to 4 weeks, whereas the untreated PTFE tubes occluded within days following implantation. In addition, vascular cell remodeling was observed in rat studies in vivo, as smooth muscle and endothelial cells migrated into and proliferated within the silk grafts, producing a confluent endothelium, a critical barrier to thrombosis.

While these results are promising, future work will need to focus on additional modifications to optimize the tube mechanics and vascular cell response. Different winding patterns or composite tubes may be generated using the gel spinning process to gain full control over geometric compliance at the sites of anastomosis, radial distension, degradation rate and overall strength. Silk grafts may be produced with and without drugs such as paclitaxel, a compound commonly used in drug-loaded stents for inhibition of vascular smooth muscle cell proliferation.<sup>19,20</sup>

This would provide more control over the vascular cell response towards matching more closely the rates of biomaterial degradation and graft remodeling.

#### Acknowledgements

The authors gratefully acknowledge funding provided by the NIH (grant EB002520) and thank Bruce Panilaitis for his help with protein adsorption studies.

#### References

1. Stegemann JP, Kaszuba SN, Rowe SL. Review: advances in vascular tissue engineering using protein-based biomaterials. *Tissue Eng* 2007; 13:2601-13.
2. Rashid ST, Fuller B, Hamilton G, Seifalian AM. Tissue engineering of a hybrid bypass graft for coronary and lower limb bypass surgery. *Faseb J* 2008; 22:2084-9.
3. Baguneid MS, Seifalian AM, Salacinski HJ, Murray D, Hamilton G, Walker MG. Tissue engineering of blood vessels. *Br J Surg* 2006; 93:282-90.
4. Kannan RY, Salacinski HJ, Edirisinghe MJ, Hamilton G, Seifalian AM. Polyhedral oligomeric silsesquioxane-polyurethane nanocomposite microvessels for an artificial capillary bed. *Biomaterials* 2006; 27:4618-26.
5. Lovett M, Cannizzaro C, Daheron L, Messmer B, Vunjak-Novakovic G, Kaplan DL. Silk fibroin microtubes for blood vessel engineering. *Biomaterials* 2007; 28:5271-9.
6. Bosiers M, Delooste K, Verbist J, Schroe H, Lauwers G, Lansink W, et al. Heparin-bonded expanded polytetrafluoroethylene vascular graft for femoropopliteal and femorocrural bypass grafting: 1-year results. *J Vasc Surg* 2006; 43:313-8.
7. Chandy T, Das GS, Wilson RF, Rao GH. Use of plasma glow for surface-engineering biomolecules to enhance bloodcompatibility of Dacron and PTFE vascular prosthesis. *Biomaterials* 2000; 21:699-712.
8. Heyligers JM, Verhagen HJ, Rotmans JJ, Weeterings C, de Groot PG, Moll FL, et al. Heparin immobilization reduces thrombogenicity of small-caliber expanded polytetrafluoroethylene grafts. *J Vasc Surg* 2006; 43:587-91.
9. Pu FR, Williams RL, Markkula TK, Hunt JA. Effects of plasma treated PET and PTFE on expression of adhesion molecules by human endothelial cells in vitro. *Biomaterials* 2002; 23:2411.
10. Lovett ML, Cannizzaro CM, Vunjak-Novakovic G, Kaplan DL. Gel spinning of silk tubes for tissue engineering. *Biomaterials* 2008; 29:4650-7.
11. Wang X, Zhang X, Castellot J, Herman I, Iafrafi M, Kaplan DL. Controlled release from multilayer silk biomaterial coatings to modulate vascular cell responses. *Biomaterials* 2008; 29:894-903.
12. Uebersax L, Mattotti M, Papaloizos M, Merkle HP, Gander B, Meinel L. Silk fibroin matrices for the controlled release of nerve growth factor (NGF). *Biomaterials* 2007; 28:4449-60.
13. Okoshi T, Soldani G, Goddard M, Galletti PM, Cohn LH. Very small-diameter polyurethane vascular prostheses with rapid endothelialization for coronary artery bypass grafting. *J Thorac Cardiovasc Surg* 1993; 105:791.
14. Haraguchi T, Okada K, Tabata Y, Maniwa Y, Hayashi Y, Okita Y. Controlled release of basic fibroblast growth factor from gelatin hydrogel sheet improves structural and physiological properties of vein graft in rat. *Arterioscler Thromb Vasc Biol* 2007; 27:548.
15. Mow VC, Huijskes R. *Basic Orthopaedic Biomechanics and Mechano-Biology*, 3<sup>rd</sup> ed. Philadelphia: Lippincott Williams & Wilkins 2005.
16. Skaggs DL, Weidenbaum M, Iatridis JC, Ratcliffe A, Mow VC. Regional variation in tensile properties and biochemical composition of the human lumbar annulus fibrosus. *Spine* 1994; 19:1310-9.
17. Chen J, Altman GH, Karageorgiou V, Horan R, Collette A, Volloch V, et al. Human bone marrow stromal cell and ligament fibroblast responses on RGD-modified silk fibers. *J Biomed Mater Res A* 2003; 67:559-70.
18. Gotoh Y, Tsukada M, Baba T, Minoura N. Physical properties and structure of poly(ethylene glycol)-silk fibroin conjugate films. *Polymer* 1997; 38:487.
19. Schiff PB, Fant J, Horwitz SB. Promotion of microtubule assembly in vitro by taxol. *Nature* 1979; 277:665-7.
20. van der Hoeven BL, Pires NM, Warda HM, Oemrawsingh PV, van Vlijmen BJ, Quax PH, et al. Drug-eluting stents: results, promises and problems. *Int J Cardiol* 2005; 99:9-17.
21. Fung YC. *Biomechanics: mechanical properties of living tissues*. 2<sup>nd</sup> Ed. New York, NY: Springer-Verlag 1993.
22. Kakisis JD, Liapis CD, Breuer C, Sumpio BE. Artificial blood vessel: the Holy Grail of peripheral vascular surgery. *J Vasc Surg* 2005; 41:349-54.
23. Bia Santana D, Armentano RL, Zocalo Y, Perez Campos H, Cabrera Fischer EI, Graf S, et al. Functional properties of fresh and cryopreserved carotid and femoral arteries and of venous and synthetic grafts: comparison with arteries from normotensive and hypertensive patients. *Cell Tissue Bank* 2006; 8:43-57.
24. Han DW, Park YH, Kim JK, Jung TG, Lee KY, Hyon SH, et al. Long-term preservation of human saphenous vein by green tea polyphenol under physiological conditions. *Tissue Eng* 2005; 11:1054-64.
25. Donovan DL, Schmidt SP, Townshend SP, Njus GO, Sharp WV. Material and structural characterization of human saphenous vein. *J Vasc Surg* 1990; 12:531-7.
26. Soffer L, Wang X, Zhang X, Kluge J, Dorfmann L, Kaplan DL, et al. Silk-based electrospun tubular scaffolds for tissue-engineered vascular grafts. *J Biomater Sci Polym Ed* 2008; 19:653.
27. Chen M, Zamora PO, Som P, Pena LA, Osaki S. Cell attachment and biocompatibility of polytetrafluoroethylene (PTFE) treated with glow-discharge plasma of mixed ammonia and oxygen. *J Biomater Sci Polym Ed* 2003; 14:917-35.
28. Jin HJ, Park J, Valluzzi R, Cebe P, Kaplan DL. Biomaterial films of *Bombyx mori* silk fibroin with poly(ethylene oxide). *Biomacromolecules* 2004; 5:711-7.
29. Bernardi B, Guidetti GF, Campus F, Crittenden JR, Graybiel AM, Balduini C, et al. The small GTPase Rap1b regulates the cross talk between platelet integrin alpha2beta1 and integrin alphaIIb beta3. *Blood* 2006; 107:2728-35.
30. Gorbet MB, Sefton MV. Biomaterial-associated thrombosis: Roles of coagulation factors, complement, platelets and leukocytes. *Biomaterials* 2004; 25:5681.
31. Nakazawa Y, Sato M, Takahashi R, Aytemiz D, Takabayashi C, Tamura T, et al. Development of small-diameter vascular grafts based on silk fibroin fibers from *Bombyx mori* for vascular regeneration. *J Biomater Sci Polym Ed* 2010; In press.